Available online at www.sciencedirect.com

ScienceDirect

Procedia CIRP 82 (2019) 154–159

www.elsevier.com/locate/procedia

17th CIRP Conference on Modelling of Machining Operations

FEM-based comparison of models to predict dynamic recrystallization during orthogonal cutting of AISI 4140

Germán González[a,*], Eric Segebade[a], Frederik Zanger[a], Volker Schulze[a]

[a] *wbk Institute of Production Science, Karlsruhe Institute of Technology (KIT), Kaiserstr. 12, 76131 Karlsruhe, Germany*

* Corresponding author. Tel.: +49-721-608-42455; fax: +49-721-608-45004. *E-mail address:* german.gonzalez@kit.edu

Abstract

Machining processes induce a thermo-mechanical load collective on the surface layer, which leads to grain refinement of varying depths depending on several factors apart from the workpiece. The size relation of the cutting edge radius to the cutting depth (relative roundness) as well as the cutting edge microgeometry influence the generation of nanocrystalline layers. In this work several models to predict dynamic recrystallization during orthogonal cutting of AISI 4140 are compared using 2D FEM-models considering both, relative roundness and cutting edge microgeometry.

Peer-review under responsibility of the scientific committee of The 17th CIRP Conference on Modelling of Machining Operations

Keywords: machining; finite element method (FEM); dynamic recrystallization

1. Introduction

Improving the surface integrity and material properties of manufactured components have been important factors in recent years for the continuous development of new production methods and advanced manufacturing technologies. Understanding the mechanisms involved in the modification of the chemical, physical and mechanical properties of the material surface during and after machining is the first step in the development of new strategies for surface characterization [1].

In material removal processes the workpiece experiences severe plastic deformations and strong temperature variations which cause defects in the material microstructure like dislocations and interfaces, and make the material thermodynamically unstable. These plastic deformations at elevated temperatures lead to a dynamic recrystallization (DRX) process and form a new grain structure in the material surface layer [2].

The presence of nanocrystalline (grain size < 100 nm) and microcrystalline grain structures (grain size < 1 µm) in the material surface layers improves its tribological and fatigue behavior, as such as its wear resistance, strength and ductility. To obtain the desired nanocrystalline layer after machining, and therefore the desired component properties, models able to predict the DRX are necessary [3-5].

The grain recrystallization of steel during machining has been studied for decades [6-8], however there is still no DRX model that clearly prevails over others and a comparative study of their accuracy has not yet been carried out.

In this research work, three DRX models for steel AISI 4140 during orthogonal cutting were compared: Zener-Hollomon [3], free Helmholtz energy [4] and dislocation density [5]. To this end, three Fortran subroutines were programmed and used in 2D FEM simulations conducted with the software Simufact Forming [9]. The influence of the asymmetrical cutting edge and relative roundness of the tools in the DRX models were also studied.

The thickness of the microcrystalline layer from the simulations were compared to experimental data [3,10] and the accuracy of each DRX model was evaluated.

2212-8271
Peer-review under responsibility of the scientific committee of The 17th CIRP Conference on Modelling of Machining Operations
10.1016/j.procir.2019.04.061

2. Case study

Orthogonal cutting process simulations were carried out for dry cutting conditions using steel AISI 4140 in a state quenched and tempered at 450 °C and uncoated cemented carbide tools with a clearance angle of α=7° and rake angle of γ=–7°. The tool microgeometries are listed in Table 1. The cutting speed v_c was set to 100 and 150 m/min.

Table 1. Cutting tool microgeometries.

N° of test	r_β/h (-)	h (µm)	r_β (µm)	K (-)	S_γ (µm)	S_α (µm)
1	0.60	50	30	1.0	-	-
2	1.00	30	30	1.0	-	-
3	1.40	50	70	1.0	-	-
4	2.20	50	110	1.0	-	-
5	2.33	30	70	1.0	-	-
6	3.66	30	110	1.0	-	-
7	-	120	-	0.2	40	200
8	-	120	-	1.0	40	40
9	-	120	-	2.0	80	40

The ratio between the cutting edge radius r_β and the uncut chip thickness h, the relative roundness r_β/h, was chosen as control parameter to follow the evolution of the grain recrystallization due to their linear relation with the grain size [3]. The Form Factor K is defined as the ratio between the cutting edge segment on the rake face S_γ and the segment on the flank face S_α [11]. Asymmetric cutting edges induce higher forces in the workpiece due to changes in the flank face edge segment due to the ploughed material on the machined surface [9].

The nanocrystalline grain structures were obtained using 2D FEM simulations and the above mentioned DRX subroutines [3-5] based on the models described in the following chapter.

3. Modeling of Dynamic Recrystallization

3.1. Zener-Hollomon empirical model

The Zener-Hollomon model defines the grain size evolution during machining as a combination of plastic deformations and temperature variations. The Zener-Hollomon parameter Z is defined as follows [2]:

$$Z = \dot{\varepsilon}_{pl} \cdot e^{\frac{Q}{R \cdot T}} \tag{1}$$

where $\dot{\varepsilon}_{pl}$ represents the strain rate, Q = 116.7 kJ/mol is the activation energy of high temperature deformation for the material, R = 8.3145 J/(K·mol) is the universal gas constant, and T is the absolute temperature in Kelvin.

The recrystallized grain size d_{DRX} is related to the Zener-Hollomon parameter according to:

$$d_{DRX} = K_1 \cdot Z^{K_2} \tag{2}$$

where K_1 and K_2 are material constants experimentally obtained. An evolution formula using the Avrami type equations and steels theory, may be combined with the Zener-Hollomon parameter to describe the kinetics of the process by dynamically recrystallized volume fraction $X^{D(0\rightarrow1)}$ [2]. The predicted resultant grain size d is a combination between the recrystallized d_{DRX}, and non-recrystallized d_0 previous grains as shown in equation 3:

$$d_{t+1} = X^{D(0\rightarrow1)} \cdot d_{DRX_t} + (1 - X^{D(0\rightarrow1)}) \cdot d_{0_t} \tag{3}$$

The dynamically recrystallized volume fraction is based on the formation of new grain boundaries due to a severe accumulated plastic strain. In order to predict the critical dynamic plastic strain, seven constants have to be incorporate to the model [3], that together with the two material constants K_1 and K_2, make a total of nine constants. Zener-Hollomon model needs a calibration phase that depends strongly on the tool geometry and workpiece. The adjustment of the model parameter is difficult because of the dynamic character of the recrystallization. Authors have followed different calibration strategies, e.g. the initial assumption of totally dynamically recrystallized volume fraction for the material parameters characterization [3] or "trial and error" procedures comparing the simulation results against the experimental values [12].

3.2. Free Helmholtz energy model

This model describes the initiation and the kinetics of the dynamic grain recrystallization considering the deformations occurred during machining as a series of highly non-isothermal and discontinuous transformations associated with changes of entropy. These changes of entropy are obtained using an analytical formulation based on the thermodynamic potential and on the free Helmholtz energy [4].

The description of the DRX as irreversible thermodynamic state changes was proposed initially by Poliak and Jonas [13] as a series of changes in von Mises strain, equivalent strain rate, temperature and grain size. Helmholtz energy f is obtained as the difference between the internal energy u and the product of the absolute temperature T and the entropy change s. The total differential of the free Helmholtz energy for a non-isothermal and irreversible process results:

$$d_f = du - s \cdot dT - T \cdot ds \tag{4}$$

The differential of the internal energy is composed of the sum of the variations of mechanical, thermal and interface energy produced by plastic work dissipation, heat conduction and grain size evolutions respectively. The changes in mechanical energy are directly related to the severe changes in plastic strain and can be obtained as the integral of the yield stress σ over the equivalent strain ε as shown in the following equation:

$$de_{mec} = \int_{\varepsilon_t}^{\varepsilon_{t+1}} \sigma(\varepsilon, \dot{\varepsilon}, T) d\varepsilon \tag{5}$$

The driving force of DRX is equal to the fraction of non-dissipated mechanical energy. In the recrystallization process interface energy is consumed. This interface energy comes from the transformation of stored mechanical energy, which describes the kinetics of DRX [4]. The final grain size can be described as:

$$d_{t+1} = \frac{3 \cdot \gamma(T)}{\frac{3 \cdot \gamma(T)}{d_t} + \Omega(T) \cdot \int (1-\beta) de_{mec}} \tag{6}$$

where $\gamma(T)$ is a parameter related to the material melting point and indicates the temperature in which the DRX starts, $\Omega(T)$ is the fraction of stored dislocation energy transformed into interface energy and β represents the fraction of dissipated mechanical energy.

3.3. Dislocation density model

This model describes the grain recrystallization as a microstructural evolution produced by the changes of the dislocation in the crystalline structures [5]. The grain microstructure is modeled as a combination of cell walls and cell interiors. The dynamic recrystallization can be obtained as the sum of the statistical and geometrically dislocations occurring in walls and interiors. The dislocation density evolution rates in cell interiors and walls are described by:

$$\begin{aligned} \dot{\rho}_c &= \alpha^* \frac{1}{\sqrt{3}b} \sqrt{\rho_w} \dot{\gamma}_w^r - \beta^* \frac{6}{bd(1-f)^{1/3}} \dot{\gamma}_c^r - k_0 \left(\frac{\dot{\gamma}_c^r}{\dot{\gamma}_0} \right)^{-1/n} \rho_c \dot{\gamma}_c^r \\ \dot{\rho}_w &= \beta^* \frac{\sqrt{3}(1-f)}{fb} \sqrt{\rho_w} \dot{\gamma}_w^r + \beta^* \frac{6(1-f)^{2/3}}{bdf} \dot{\gamma}_c^r - k_0 \left(\frac{\dot{\gamma}_w^r}{\dot{\gamma}_0} \right)^{-1/n} \end{aligned} \tag{7}$$

where the cell interior dislocation density is defined as ρ_c and the dislocation density in the cell walls is defined as ρ_w. The dislocation density evolution rate control parameters e.g. the dynamic coefficient of dislocation generation α^*, the integration between the cell walls and interiors β^* and dislocation annihilation k_0 must be determined by model calibration.

3.4. Material model

The workpiece deformation behavior was simulated using a Voce-constitutive based material model [14]. The flow stress σ, depends on the plastic strain ε_{pl}, the strain rate $\dot{\varepsilon}_{pl}$ and the temperature T, and was defined as [15]:

$$\sigma = \underbrace{\sigma_0^* \cdot \left(1 - \left(\frac{T}{T_0} \right)^n \right)^m}_{\sigma^*} + \underbrace{\left(\sigma_{G0} + \left(\sigma_1 + \theta_1 \cdot \overline{\varepsilon_p} \right) \cdot \left(1 - \exp\left(- \frac{\theta_1 \cdot \overline{\varepsilon_p}}{\theta_0} \right) \right) \right) \cdot \frac{G(T)}{G(0K)} \cdot g\left(T, T_{tr}\right)}_{\sigma_G} \tag{8}$$

where σ^* and σ_G are the athermal and thermal component respectively, $G(T)$ is the shear modulus, $g(T)$ describes the temperature of softening and n, m, σ_1, θ_0 and θ_1 are material parameters obtained experimentally for AISI 4140 [10].

4. FE-Model set-up

The 2D FEM simulations were performed using the commercial software Simufact Forming. The simulation components, as shown in Figure 1, were a rigid tool fixed in the space, an elasto-plastic workpiece, an elastic body, a holder and a heat sink.

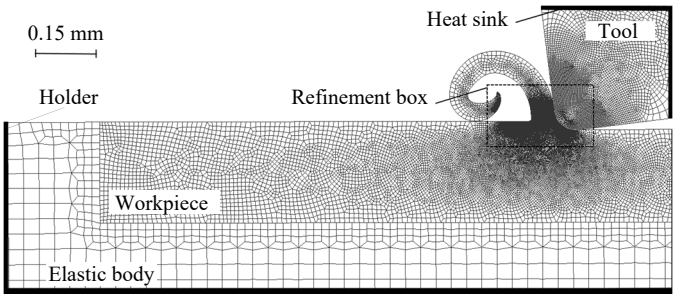

Fig. 1. 2D finite element process model of orthogonal cutting

The selected mesh type uses quadrilateral elements in plane strain condition with continuous remeshing depending on refinement boxes featuring local refinement [9]. The software offers forging press kinematics, thus the holder imitates a hydraulic press with constant velocity in the opposite direction of cut. DRX and material models were used to obtain the dynamic grain refinement and the workpiece deformations. The friction of the system was described using a temperature independent combined Coulomb-shear friction model. The Coulomb factor value μ and the shear factor value m were fixed at 0.35 and 0.70 respectively [9].

4.1. Steady State

To determine properly the micro- and nanocrystalline grain structures after the recrystallization process the size of the workpiece elements of the FE simulations have to be small enough. Moreover the simulated process has to achieve the steady state. Therefore, simulations may be highly time consuming. In order to minimize the calculation time, reaching the steady state as quickly as possible while maintaining the accuracy of the results, the presented strategy consisting in a series of four simulations was followed:

- In the first simulation an approximation of the steady state temperature of the cutting tool was obtained. The aim of this simulation, as well as of the second and third simulations, is to determine the steady state values of temperature and strain rate, thus the DRX model used does not affect to the results. An initial cutting path of 1.50 mm was simulated. The initial minimum element edge length of the workpiece and tool were 5 and 3 µm respectively. The heat transfer coefficient of the workpiece with the environment was 50 W/(m^2·K). The cutting tool was glued to a heat sink

element, the thermal conductivity was set to 80 W/(m·K) and the specific heat capacity was fixed at 2.3e-7 J/(kg·K).

- In the second simulation a cutting path of 0.50 mm was simulated in a new workpiece with a minimum element edge length of 2.5 µm. The initial temperature of the cutting tool was set equal to the temperature of the tool at the end of the first simulation using the same mesh. The tool specific heat capacity was set very high for maintaining the tool temperature constant during machining. In this simulation the approximated steady state values of the workpiece, temperature and strains, were determined.
- In the third simulation a cutting path of 1.00 mm was simulated starting from the end of the path of the second simulation resulting in a total simulated distance of 1.50 mm. The minimum element edge length of the workpiece was reduced to 1 µm. The initial temperature and strain values of both, tool and workpiece were set equal to the values at the end of the second simulation. The tool specific heat capacity coefficient was set according to a real case at 230 J/(kg·K) [12]. The steady state was achieved at the end of the simulation resulting an almost constant tool temperature throughout the cut.
- In the fourth simulation the thickness of the micro- and nanocrystalline layer was obtained using each of the three selected DRX models, thus this simulation was carried out three times. The steady state values of tool and workpiece obtained in the previous simulation were used as input for both tool and workpiece initial state. A cutting path of 0.25 mm was simulated starting from the end of the path of the third simulation resulting in a total path of 1.75 mm. The mesh of the workpiece was refined up to 0.5 µm. An initial grain size of d_0=5 µm was used for the three DRX subroutines.

With this simulation strategy, the number of simulations needed, as well as the calculation time, were considerably reduced.

5. Results and discussion

The thickness of the nanocrystalline layers after the cutting processes described in chapter 2, were determined using 2D FEM simulations based on three dynamic recrystallization models explained in chapter 3 which followed the steady state strategy reported in chapter 4. Figure 2 shows the workpiece grain size d during the simulations of the test number 2 carried out with a cutting speed of 100 m/min and using the dislocation density subroutine.

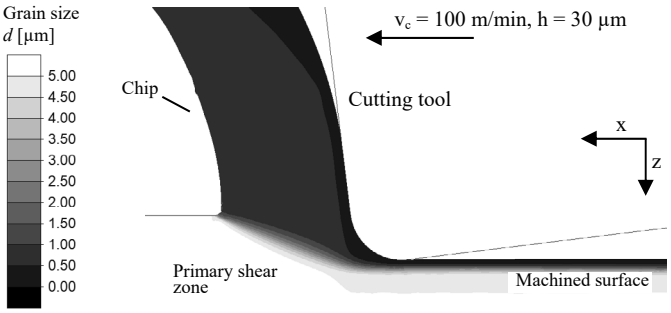

Fig. 2. FEM result of the surface layer microstructure during machining of AISI 4140 using dislocation density subroutine, r_β/h=1 and K=1

The simulation predicts a total recrystallization of the chip, which does not usually occur in experiments. The model can thus only be used to predict the nanocrystalline layer depth, and not the underlying mechanisms. In order to compare the results of the simulations with the available experimental data [3,10], the depth of the microcrystalline layer with grain size smaller than 1 µm $z_{d=1\mu m}$ was determined and listed in Table 2. Note that the test numbers correspond to the geometrical tool characteristics listed in Table 1.

Table 2. Experimental and simulation results, v_c = 100 m/min.

N° of test	Experimental $z_{d=1\mu m}$ (µm)	Zener-Hollomon $z_{d=1\mu m}$ (µm)	Helmholtz Energy $z_{d=1\mu m}$ (µm)	Dislocation Density $z_{d=1\mu m}$ (µm)
1	4.10 [1]	5.20	4.50	4.20
2	5.10 [1]	4.30	3.80	3.95
3	4.80 [1]	9.70	8.10	5.30
4	6.00 [1]	10.80	10.40	5.80
5	6.40 [1]	6.70	7.60	5.50
6	7.00 [1]	8.60	7.00	6.30
7	2.50 [2]	13.25	13.10	7.40
8	2.00 [2]	8.60	7.30	5.70
9	1.80 [2]	7.50	7.60	5.50

[1]: data from [3], [2]: data from [10]

Figure 3 presents the experimental [3] and simulation results of the six first tests listed in Table 2 against the relative roundness r_β/h. In general, the thickness of the microcrystalline layer increases with the relative roundness.

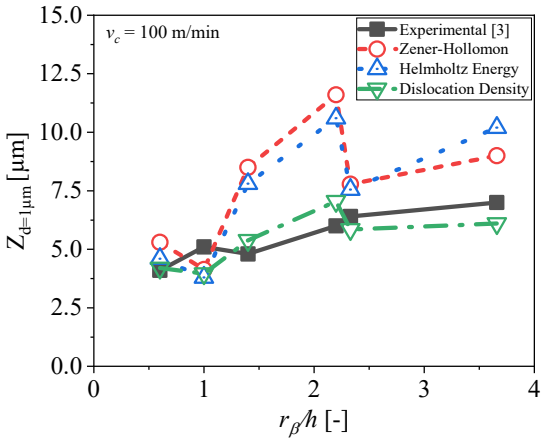

Fig. 3. Comparison of simulation and experimental results. v_c = 100 m/min. Symmetric cutting edges

The dislocation density model obtained more accurate results for the major range of tests than the other two methods. Some points move away from the expected trajectory but their effects may not be weighted.

Figure 4 shows the experimental [10] and simulation results of the tests 7 to 9 carried out using tools with asymmetric edges. It has to be considered that the experimental results used in this work come from different sources and the DRX model parameters were fitted using only one of them [3]. This may lead to deviations in the simulation results.

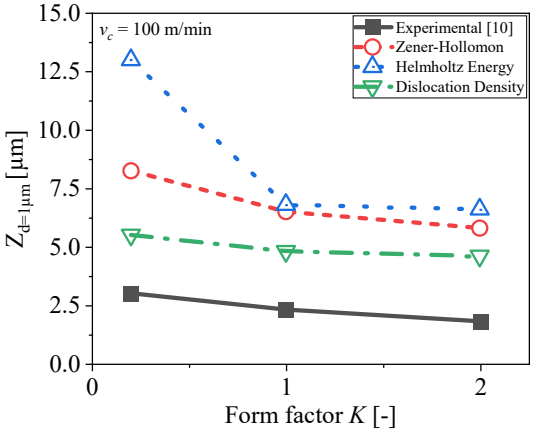

Fig. 4. Comparison of simulation and experimental results. v_c = 100 m/min. Asymmetric cutting edges

All the results of Figure 4 show the same tendency, the thickness of the microcrystalline layers decrease with a greater form factor. In this series of tests the dislocation density model is again the most reliable of the three DRX studied models.

The analyzed field was expanded to higher cutting speeds using the simulations. The cutting speed was increased to 150 m/min. The results of the simulations are listed in Table 3.

Table 3. Simulations results, v_c = 150 m/min.

N° of test	Zener-Hollomon $z_{d=1\mu m}$ (µm)	Helmholtz Energy $z_{d=1\mu m}$ (µm)	Dislocation Density $z_{d=1\mu m}$ (µm)
1	4.90	4.60	4.10
2	4.60	4.10	3.75
3	8.40	8.20	5.90
4	11.00	11.10	7.80
5	7.40	7.20	5.33
6	8.20	7.80	6.90
7	11.10	11.00	8.80
8	10.20	7.75	5.60
9	10.10	9.40	7.60

Figures 5 and 6 present the simulation results listed in Table 3 considering r_β/h and Form Factor K.

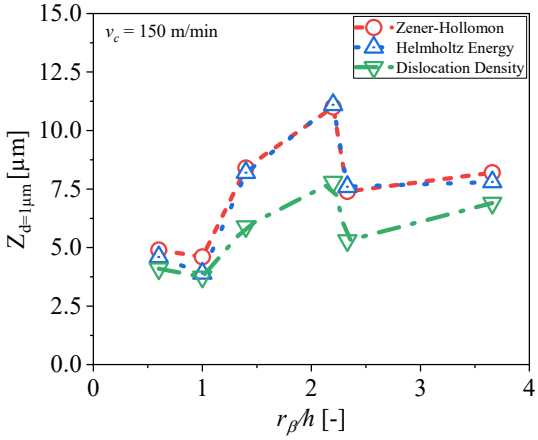

Fig. 5. Simulation results. v_c = 150 m/min. Symmetric cutting edges

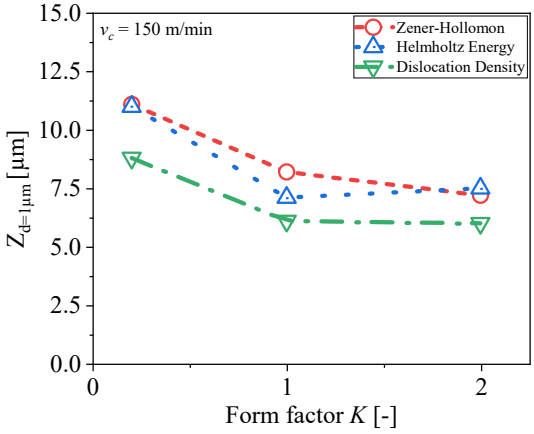

Fig. 6. Simulation results. v_c = 150 m/min. Asymmetric cutting edges

With an increase of the cutting speed, the thickness of the microcrystalline layer increases slightly.

Although no experimental results were available to make a comparison, the results of the simulations represented the expected trends [10,15]

6. Conclusions

In this research work, a comparative study of three models for dynamic grain recrystallization (DRX) prediction during machining was carried out. The studied models were Zener-Hollomon, free Helmholtz energy and dislocation density.

Using 2D FEM simulations and the above mentioned DRX models, the microcrystalline layers presented on the machined surfaces were predicted and compared with experimental data. The FEM simulations were conducted using the software Simufact Forming.

The cutting process used in the analysis was an orthogonal cutting operation on AISI 4140 with uncoated carbide tools using symmetric and asymmetric microgeometries. The effects of the tool microgeometry on the DRX models was also investigated.

It was determined that the tool set up with bigger relative roundness on the cutting edge produce thicker microcrystalline layers on the machined surface of AISI 4140.

Tools with bigger Form Factor generate thinner microcrystalline layers and an increment in the cutting speed lead to an increment in the microcrystalline layer thickness.

The comparisons of the 2D FEM results with the experimental data determined that the most accurate DRX model for this case study is the dislocation density model.

In further investigations, the precision of the models using 3D FEM simulations will be analyzed.

Acknowledgements

The scientific work has been supported by the DFG within the research priority program SPP 2086. The authors thank the DFG for this funding and intensive technical support.

References

[1] Jawahir IS, Brinksmeier E, M'Saoubi R, Aspinwall D, Outeiro J, Meyer D, Umbrello D, Jayal AD. Surface integrity in material removal processes: recent advances. CIRP Annals-Manufacturing Technology 2011; 60:603-626.

[2] Yanagimoto J, Karhausen K, Brand AJ, Kopp R. Incremental Formulation for the Prediction of Flow Stress and Microstructural Change in Hot Forming. ASME. J. Manuf. Sci. Eng. 1998; 120:316-322.

[3] Ambrosy F, Zanger F, Schulze V. FEM-simulation of machining induced nanocrystalline surface layers in steel surfaces prepared for tribological applications. CIRP Annals- Manufacturing Technology 2015; 64:69-72.

[4] Buchkremer S, Klocke F. Modeling nanostructural surface modifications in metal cutting by an approach of thermodynamic irreversibilityDerivation and experimental validation. Continuum Mechanics and Thermodynamics 2017; 29:271-289.

[5] Ding H, Shin YC. Dislocation Density-Based Grain Refinement Modeling of Orthogonal Cutting of Titanium. ASME. J. Manuf. Sci. Eng. 2014; 136:041003-11.

[6] Swaminathan S, Shankar MR, Lee S, Hwang J, King AH, Kezar RF, Rao BC, Brown TL, Chandrasekar S, Compton WD, Trumble KP. Large Strain Deformation and Ultra-Fine Grained Materials by Machining. Mater. Sci. Eng. 2005; 410-411.

[7] Shankar MR, Verma R, Rao BC, Chandrasekar S, Compton WD, King AH, Trumble KP. Severe Plastic Deformation of Difficult-to-Deform Materials at Near-Ambient Temperature. Proceedings of Metallurgical and Materials Transactions: Physical Metallurgy and Materials Science, Springer, Boston. 2007;1899-1905.

[8] Deng WJ, Xia W, Li C, Tang Y. Ultrafine Grained Material Produced by Machining. Materials and Manufacturing Processes. 2010;25:355-359.

[9] Segebade E, Gerstenmeyer M, Zanger F, Schulze V. Cutting simulations using a commercially available 2D/3D FEM software for forming. Procedia CIRP 2017; 58:73-78.

[10] Gerstenmeyer M. Entwicklung und Analyse eines mechanischen Oberflächenbehandlungsverfahrens unter Verwendung des Zerspanungswerkzeuges. Karlsruhe Institute of Technology, Dissertation, 2018.

[11] Denkena B, Biermann D. Cutting edge geometries. CIRP Annals-Manufacturing Technology 2014; 63:631–653.

[12] Rotella G et al. Finite Element Modeling of Microstructural Changes in Turning of AA7075-T651 Alloy. Journal of Manufacturing Processes, 2013; 156.1.1.1.:87-95.

[13] Poliak. E.I., Jonas J.J. A one-parameter approach to determining the critical conditions for the initiation of dynamic recrystallization. Acta Mater. 1996; 44:127-136.

[14] Voce E. The relationship between stress and strain for homogeneous deformation. Journal of the Institute of Metals 1948; 74:537-562.

[15] Authenrieth H. Numerische Analyse der Mikrozerspanung am Beispiel von normalisiertem C45E. Karlsruhe Institute of Technology, Dissertation, 2010.